

# Internal B–O Bond-Facilitated Photoisomerization of Boranes: Ring Expansion Versus Oxyborane Elimination/Intramolecular Diels–Alder Addition

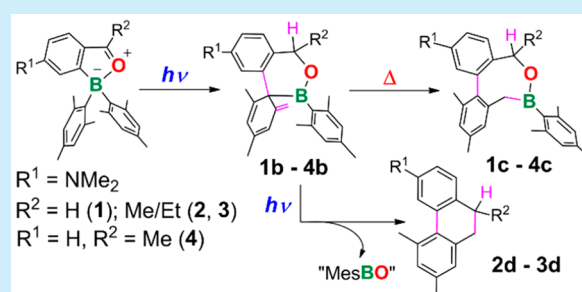
Guo-Fei Hu,<sup>†</sup> Hai-Jun Li,<sup>‡</sup> Chao Zeng,<sup>†</sup> Xiang Wang,<sup>‡</sup> Nan Wang,<sup>†</sup> Tai Peng,<sup>†</sup> and Suning Wang<sup>\*,†,‡,§</sup>

<sup>†</sup>Laboratory of Cluster Science, Ministry of Education of China, Beijing Key Laboratory of Photoelectronic/Electrophotonic Conversion Materials, School of Chemistry and Chemical Engineering, Beijing Institute of Technology, Beijing, China

<sup>‡</sup>Department of Chemistry, Queen's University, Kingston, Ontario K7L 3N6, Canada

**S** Supporting Information

**ABSTRACT:** Boron compounds (1–4) containing an internal B–O bond have been found to undergo facile multistructural transformations upon irradiation at 365 or 410 nm, generating rare 8-membered B,O-heterocycles (1c–4c). In addition, 2 and 3 also undergo an intramolecular Diels–Alder addition and oxyborane elimination concomitantly, via intermediates 2b/3b, producing 2d/3d. The pathways to isomer c and product d were found to be a thermal process and a photo process, respectively.



Boron-supported substrates are widely used in chemical modification and synthesis.<sup>1</sup> A variety of bond formations facilitated by a boron unit are well-known in the literature.<sup>2,3</sup> Metal-free coupling reactions and other chemical reactions facilitated by boron have attracted much research attention.<sup>2,3</sup> Recent studies on photoisomerization of boranes, especially those of triarylboranes and their derivatives, demonstrated the possibility of using light to achieve the rare intramolecular structural transformation of boranes.<sup>4</sup> Photochemical transformation of internal-donor-supported four-coordinated boranes often leads to rare and functional boron heterocycles in a quantitative manner that are difficult to access via conventional approaches.<sup>5</sup> Most previously studied photoreactive four-coordinate borane systems rely on an aryl or a heteroaryl moiety as such pyridyl or thiazolyl as the supporting donor to boron (type I in Figure 1<sup>6b</sup> and Scheme 1a).<sup>6</sup> For a longtime, such diaryl chelate units were thought to be necessary in order to achieve structural integrity throughout the photoreaction and intramolecular charge transfer (CT) from Ar to the chelate, which initiates the photoisomerization. Recently the

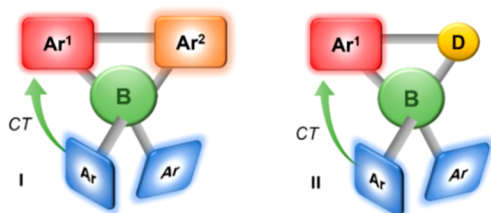
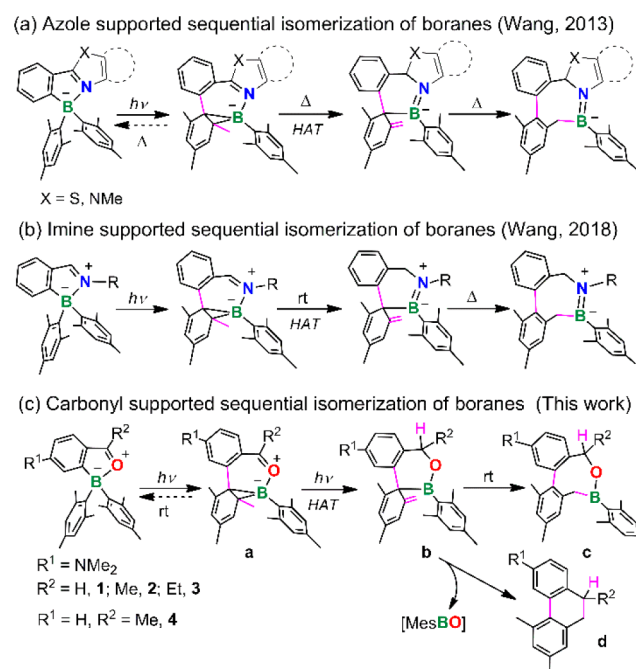


**Figure 1.** Type I and II photochromic four-coordinated borane systems.

## Scheme 1. (a) Azole, (b) Imine, and (c) Carbonyl-Supported Photoreactive Borane Systems



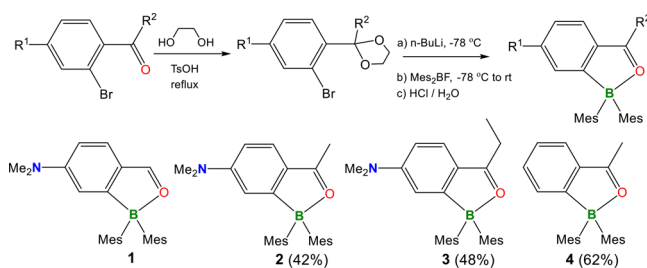
imine-supported type II system in Scheme 1b was found to undergo a highly efficient photoisomerization, following a

Received: June 2, 2019

similar pattern as does the type I analogue,<sup>7</sup> illustrating that a simple conjugated donor is capable of supporting borane phototransformation. The strong electron-donating ability of the imine group was thought to play an important role in the efficient photoisomerization of the imine-supported system. To expand the scope of the type II photoreactive system, we studied a carbonyl-supported borane system (Scheme 1c). The O atom on a carbonyl is a much weaker donor to boron, compared to the imine N atom. Therefore, it is very surprising that the carbonyl-supported molecules were found to display a similar phototransformation as the imine analogues and are much more reactive toward light with divergent reaction pathways. In addition to the formation of B,O-heterocycles (c), unusual elimination of oxyborane (MesBO) and the formation of species d, which is a rare carbonyl to alkane conversion product, was also observed. The details of these interesting new findings are presented herein.

Compounds 1–4 were prepared in good yields, according to the general procedure shown in Scheme 2. Compound 1 is a

### Scheme 2. Synthetic Procedures for Compounds 1–4



previously known molecule used as a precursor molecule for a donor–acceptor functionalized stilbene that we recently reported.<sup>8</sup> The introduction of the NMe<sub>2</sub> para to the aldehyde/keto group in 1–3 is to enhance the nucleophilicity of the carbonyl group. The variation of the R<sup>2</sup> group from H atom to ethyl is for the purpose of examining the impact of both electronic and steric factors on the photoreactivity of this class of compounds and the possibility of converting the carbonyl to a stereogenic center via photoisomerization. To compare the impact of the amino group, molecule 4, which lacks the *p*-amino group with R<sup>2</sup> = methyl was also prepared. Full characterization details for compounds 2–4 are provided in the Supporting Information.

The <sup>11</sup>B NMR chemical shifts of 1–4 in benzene are 13.6, 13.5, 13.4, and 16.3 ppm, respectively, supporting their four-coordinate structures in solution. The ~3 ppm difference of the <sup>11</sup>B NMR signal between 2 and 4 indicates that the *p*-NMe<sub>2</sub> group indeed enhances the keto-donating ability to the B center. Replacing the H atom on the R<sup>2</sup> site by a methyl or an ethyl group appears to have little effect on the electron density on boron. It is noteworthy that the isomer of 1 with the NMe<sub>2</sub> group being para to BMes<sub>2</sub> and meta to the aldehyde is three-coordinated with a <sup>11</sup>B NMR signal at ~60 ppm, and is not photochemically active.<sup>9</sup> Therefore, the location of the amino group is important in modulating the structure and the properties of this class of borane molecules. The crystal structures of 1–3 were determined by X-ray diffraction (XRD) analyses. Their B–O bond lengths are similar (1.607(2), 1.612(6), and 1.624(4) Å for 1–3, respectively; see the Supporting Information (SI)).

The absorption spectra of 1–3 have a broad and intense band near 400 nm ( $\lambda_{\max} = 397$  nm (1);  $\lambda_{\max} = 388$  nm (2 and 3)), whereas, in contrast, compound 4 has a very weaker band at a much lower energy ( $\lambda_{\max} = 412$  nm), as shown in Figure 2. The NMe<sub>2</sub> unit on the chelate backbone is clearly responsible for the intense absorption bands of 1–3.

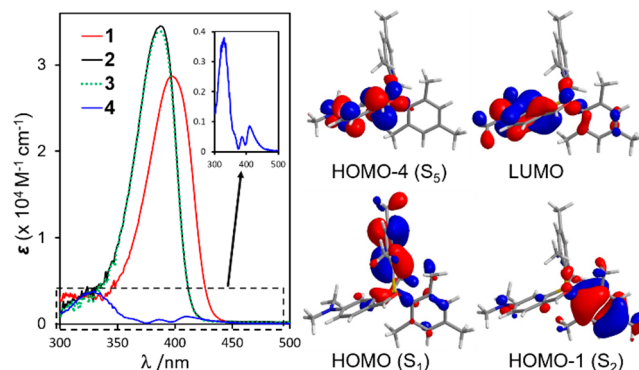


**Figure 2.** Absorption spectra of 1–4 in toluene ( $1.0 \times 10^{-5}$  M, left) and the diagrams of key orbitals involved in vertical excitations to S<sub>1</sub>, S<sub>2</sub>, and S<sub>5</sub> states of 1 (right). Inset shows an enlarged absorption spectrum of 4.

To elucidate the origin of the absorption spectra, time-dependent density functional theory (TD-DFT) calculations (B3LYP/6-31G(d)) for 1, 2, and 4 were performed; the details are given in the SI. For 1 and 2, the vertical excitations to the S<sub>1</sub> states (HOMO (H) to LUMO (L), 98%–99%,  $f = 0.0087$ , 0.0089) and the S<sub>2</sub> states (H-1 to L, 96%–97%,  $f = 0.0256$ , 0.0246) are similar in energy with appreciable oscillator strengths, and can be ascribed to charge transfer (CT) transitions from the Mes groups to the chelate backbone (Figure 2). The vertical excitations to the S<sub>3</sub> and S<sub>4</sub> states of 1/2 are similar CT transitions involving H-2 (98%) and H-3 to L (97%), respectively, but much smaller oscillator strengths (0.0008 and 0.0025–0.0027). The vertical excitation to the S<sub>5</sub> state is mainly a  $\pi \rightarrow \pi^*$  (H-4 to L, > 83%) localized on the chelate backbone, with the amino to the carbonyl CT character, and a very large oscillator strength (0.3621 and 0.3677 for 1 and 2, respectively). The orbitals involved in vertical excitations to the S<sub>1</sub> to S<sub>5</sub> states for 4 are similar to those of 1 and 2, except they lack the amino group, and the transitions having very small oscillator strengths. The calculated trend of vertical excitation energies to S<sub>1</sub> and S<sub>2</sub> states for 1, 2, and 4 matches well that observed in the absorption spectra. Compounds 1–4 are weakly emissive with  $\lambda_{\text{em}} \approx 540$  nm for 1,  $\lambda_{\text{em}} \approx 520$  nm for 2 and 3, and  $\lambda_{\text{em}} \approx 570$  nm for 4, and a large Stokes shift (>100 nm; see the SI). The fact that the S<sub>1</sub>–S<sub>4</sub> states for all four compounds are CT transitions from Mes to the chelate backbone is important, because such CT transitions drive the photoisomerization of donor-supported chelate borane systems.<sup>6,7</sup>

Compounds 1–4 are all responsive to irradiation at 365 nm (1–3) or 410 nm (4), undergoing quantitative isomerization, reaching completion in ~2 h (0.05 M in C<sub>6</sub>D<sub>6</sub>), as shown by the NMR spectral tracking data (see the SI). At low temperature (–78 °C), upon irradiation, compounds 1–4 transform to dark-colored species 1a–4a, which most likely possess structures similar to the boratanorcaradiene (borirane) isomers a, identified for the azole- or imine-supported systems, shown in Figure 3. Similar to the imine analogues, 1a–4a are

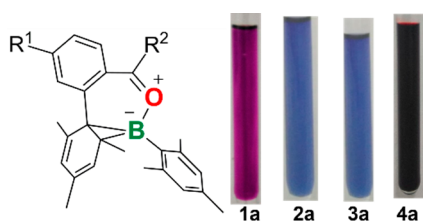


**Figure 3.** Proposed structure and photographs of **1a–4a** in benzene, taken immediately after the NMR tubes irradiated by UV light (365 nm) were pulled out of the dry ice bath.

thermally unstable. However, unlike the imine analogues **a**, which can be characterized by NMR at low temperature and converted to the H-atom transfer (HAT) isomer **c** at room temperature (rt), **1a–4a** could not be characterized by NMR, because of their rapid reversal back to **1–4** at temperatures above  $-40\text{ }^{\circ}\text{C}$ .

When the photoreaction is performed at ambient temperature, **1–4** isomerize rapidly to **1b–4b**, respectively, which were observed in the  $^1\text{H}$  NMR spectra, albeit short-lived (see Figure 6, presented later in this work). Therefore, the **a**  $\rightarrow$  **b** isomerization for the carbonyl-supported system is driven by light. **1b–4b** further isomerize to **1c–4c**, forming the ring-expansion products, which are similar to the imine analogues and fully characterized by nuclear magnetic resonance (NMR), high-resolution mass spectroscopy (HRMS), and XRD analyses (**3c** and **4c**; see Figure 4). For **1** and **4**, the formation

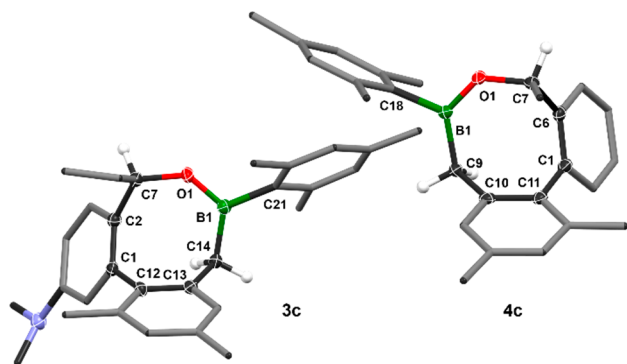


**Figure 4.** Crystal structures of **3c** and **4c** with H atoms omitted for clarity. Selected bond lengths for **3c**: B1–O1, 1.369(8) Å; B1–C14, 1.584(9) Å; B1–C21, 1.571(8) Å; and O1–C7, 1.451(7) Å. Selected bond lengths for **4c**: B1–O1, 1.348(6) Å; B1–C9, 1.579(6) Å; B1–C18, 1.579(6) Å; and O1–C7, 1.454(6) Å.

of the **c** isomer is quantitative. **1c** is identified by its characteristic methylene groups ( $\text{CH}_2\text{--O}$  and  $\text{CH}_2\text{--B}$ ), showing two sets of AB splitting patterns, because of the unsymmetrical structure. The  $\text{CH}_2\text{--B}$  in **4c** displays an AB splitting pattern similar to that of **1c**, while the H atom and the  $\text{CH}_3$  group on the chiral C7 atom display a quartet and a doublet splitting pattern, respectively (see the SI). Significantly, no diastereomer peaks were observed in the  $^1\text{H}$  NMR spectrum of **4c**, indicating that the HAT step is stereoselective, similar to that observed in the azoly-supported system in Scheme 1a. **1c** and **4c** have a broad  $^{11}\text{B}$  NMR peak at  $\sim 52$  ppm (Figure 5), which is  $\sim 7$  ppm downfield from those of the imine analogues; this is a reflection of a reduced donor strength of the carbonyl group. As shown in Figure 4, the 8-membered rings in **3c** and **4c** have an approximate boat structure. The B–

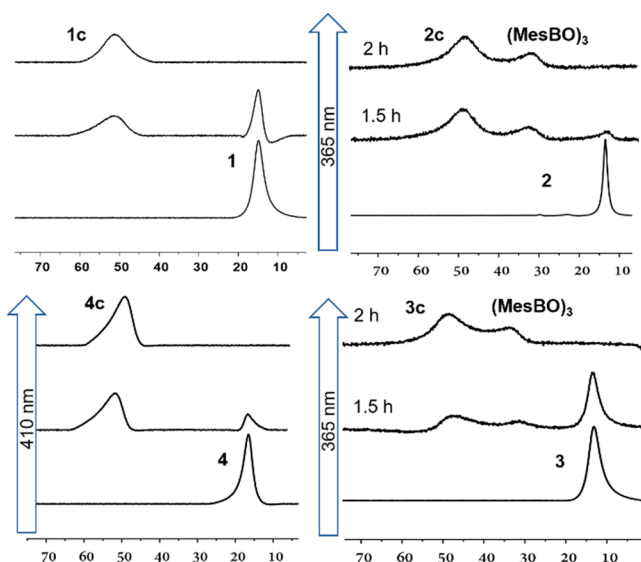


**Figure 5.**  $^{11}\text{B}$  NMR spectra showing the photoconversion of **1–4** (0.05 M in  $\text{C}_6\text{D}_6$ ).

O bonds in **3c** and **4c** are quite short, 1.369(8) and 1.348(6) Å, respectively, which is an indication of the presence of a partial  $\pi$ -bond between the B and O atoms.<sup>10</sup> The most important feature of **3c** and **4c** is the stereogeometry of the chiral C7 atom. Consistent with those observed in the azole-supported system, the H atom on the C7 atom of **3c** and **4c** is *syn* to the C–C bond of the neighboring benzene ring, while the *anti*-diastereomer was not observed. This further supports that the HAT process in the carbonyl-supported system is a concerted intramolecular process, following the same mechanistic pathway as the azole-supported borane system.<sup>6b</sup> Compounds **1c–4c** are air-stable and thermally stable. Heating their toluene solutions to  $100\text{ }^{\circ}\text{C}$  did not produce any obvious change of their NMR spectra.

Interestingly, for **2** and **3**, in addition to the formation of **2c** and **3c**, which have a  $^{11}\text{B}$  NMR peak at  $\sim 48$  and  $\sim 50$  ppm, respectively (Figure 5), a new species **2d/3d** was also observed in the photoreaction mixture, formed concomitantly with **2c/3c**, as shown by Figure 6. Furthermore, a distinct  $^{11}\text{B}$  NMR peak at  $\sim 33$  ppm was observed for the photoreaction of **2/3**, which was identified as a boroxine ( $\text{MesBO}$ )<sub>3</sub> (see Figure S6F in the SI).<sup>11</sup> **2c** and **3c** were separated from the products by crystallization (NMR yields for both compounds are  $\sim 70\%$ ; isolated yields are  $\sim 50\%$ ), while **2d** and **3d** were isolated by column chromatography as colorless oils in 15% and 21% yield, respectively. HRMS and 2D NMR spectroscopic analyses established that **2d** and **3d** are *N,N*,5,7,10-pentamethyl-9,10-dihydro-phenanthren-3-amine and 10-ethyl-*N,N*,5,7-tetramethyl-9,10-dihydrophenanthren-3-amine, respectively, as shown in Figure 6.

Mechanistically, **2c/3c** is formed via a 1,3-sigmatropic shift of the BMes unit in **2b/3b** (the red pathway) similar to that established previously for azole- and imine-supported systems.<sup>6b,7</sup> **2d/3d** is likely formed via a retro-Diels–Alder process, eliminating a MesBO unit, followed by an intramolecular Diels–Alder cycloaddition of the vinyl group to the chiral atom in **2b/3b** (the blue pathway). Oxyboranes that are not stabilized by an internal donor (e.g., an O,X-chelate) and an acid are highly unstable and readily undergo dimerization or trimerization, forming boroxine-like species.<sup>12</sup> Therefore, the

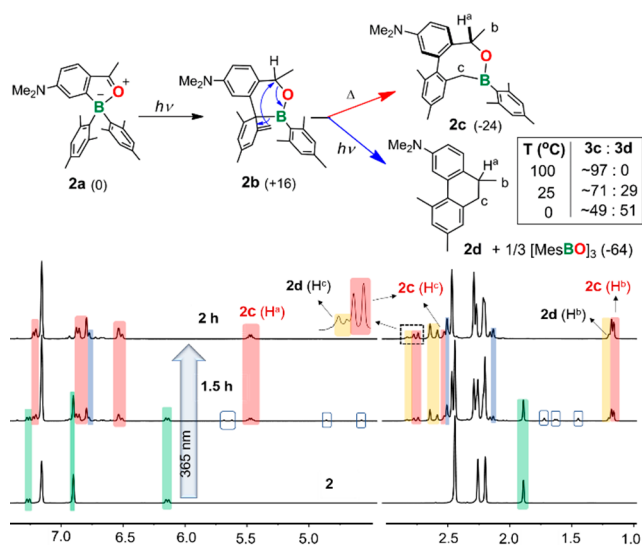


**Figure 6.** (Top) Scheme showing the two competing isomerization pathways of **2**, the DFT calculated energy (kcal/mol, B3LYP/6-31G(d), relative to **2**) and the ratio of **3c**:**3d** observed by NMR for photoreactions at different temperatures. (Bottom)  $^1\text{H}$  NMR spectra showing the photoconversion of **2** (green)  $\rightarrow$  **2b** (blue box)  $\rightarrow$  **2c** (red)/**2d** (yellow) +  $(\text{MesBO})_3$  (blue) in  $\text{C}_6\text{D}_6$ , (0.05 M). (The vertical scale of the two top spectra was increased to show some of the small peaks.)

isolation of  $(\text{MesBO})_3$  is consistent with the generation of oxyborane in the photoreaction of **2** and **3**. The fact that oxyborane elimination was not observed for **1** and **4** could be attributed to the lack of a R group in **1** and an *p*- $\text{NMe}_2$  group in **4**, which reduces the electron density on the C atom bound to the O atom, making the departure of the oxyborane in **1b** and **4b** more difficult, compared to that in **2b** and **3b**. The relative thermodynamic stability of different species involved in the transformation of **2** was examined by DFT computational analysis and shown in Figure 6. The products formed via either the red or blue pathways are all thermodynamically favored, compared to **2**. The relatively higher distribution of **2c** in the products may be caused by a smaller activation barrier for the red pathway, relative to the blue pathway, if both pathways were thermal processes. To verify this, the photoreactions of **2** and **3** were repeated at 100 and 0 °C, respectively. Surprisingly, **2c**/**3c** was obtained as a clean product at 100 °C, while the yield of **2d**/**3d** increased substantially at 0 °C (see the box in Figure 6, as well as Figure S3X in the SI). This led us to suggest that the red pathway forming **c** is a thermal process, while the blue pathway, forming **d** and oxyborane/boroxine, is a photochemical pathway, which is likely initiated by the rupture of the C–O bond in **2b**. The fact that the imine-supported system does not undergo a similar deborylation process may be explained by the relatively high propensity of benzylic C–O bonds toward photochemical cleavage.<sup>13</sup>

Lastly, qualitative comparison of the overall isomerization rates of the azole-, imine-, and carbonyl-supported systems to the final isomer **c** (for >80% conversion) indicate that the isomerization reactivity follows the order of carbonyl (~2 h at rt, 365 nm/410 nm) > imine (~16 h at rt, 365 nm) > azole (e.g., benzothiazole, ~12 h at 50 °C, 365 nm). Hence, a carbonyl donor appears to enhance the photoreactivity of four-coordinated boranes greatly. Further investigation is underway

to fully understand the role of the carbonyl group in the facile phototransformation of borane compounds.

## ■ ASSOCIATED CONTENT

### Supporting Information

The Supporting Information is available free of charge on the ACS Publications website at DOI: 10.1021/acs.orglett.9b01892.

Synthetic details, characterization data, TD-DFT data, photo and thermal elimination experiments, UV-vis spectra, and crystal data of **1**–**4** (PDF)

## Accession Codes

CCDC 1916845–1916849 contain the supplementary crystallographic data for this paper. These data can be obtained free of charge via [www.ccdc.cam.ac.uk/data\\_request/cif](http://www.ccdc.cam.ac.uk/data_request/cif), or by emailing [data\\_request@ccdc.cam.ac.uk](mailto:data_request@ccdc.cam.ac.uk), or by contacting The Cambridge Crystallographic Data Centre, 12 Union Road, Cambridge CB2 1EZ, UK; fax: +44 1223 336033.

## ■ AUTHOR INFORMATION

### Corresponding Author

\*E-mail: [sw17@queensu.ca](mailto:sw17@queensu.ca).

### ORCID

Nan Wang: 0000-0001-5973-4496

Suning Wang: 0000-0003-0889-251X

### Notes

The authors declare no competing financial interest.

## ■ ACKNOWLEDGMENTS

We thank the National Natural Science Foundation of China for financial support (Grant Nos. 21571017, 21701011, and 21761132020) and the Natural Science and Engineering Research Council of Canada (No. RGPINI-2018-03866). We are also grateful to Compute Canada for the use of their computational facilities.

## ■ REFERENCES

- (1) *Boronic Acids: Preparation, Applications in Organic Synthesis and Medicine*; Hall, D. G., Ed.; Wiley-VCH: Weinheim, Germany, 2005.
- (2) (a) Jupp, A. R.; Stephan, D. W. New Directions for Frustrated Lewis Pair Chemistry. *Trends in Chemistry* **2019**, *1*, 35–48. (b) Légaré, M. A.; Bélanger-Chabot, G.; Dewhurst, R. D.; Welz, E.; Krummenacher, I.; Engels, B.; Braunschweig, H. Nitrogen fixation and reduction at boron. *Science* **2018**, *359*, 896–900. (c) Légaré, M.-A.; Courtemanche, M.-A.; Rochette, E.; Fontaine, F. G. Metal-free catalytic C–H bond activation and borylation of heteroarenes. *Science* **2015**, *349*, 513–516. (d) Stephan, D. W.; Erker, G. Frustrated Lewis pair chemistry: development and perspectives. *Angew. Chem., Int. Ed.* **2015**, *54*, 6400–6441. (e) Mahdi, T.; Stephan, D. W. Frustrated Lewis pair catalyzed hydroamination of terminal alkynes. *Angew. Chem., Int. Ed.* **2013**, *52*, 12418–12421.
- (3) (a) Noda, H.; Furutachi, M.; Asada, Y.; Shibasaki, M.; Kumagai, N. Unique physicochemical and catalytic properties dictated by the  $\text{B}_3\text{NO}_2$  ring system. *Nat. Chem.* **2017**, *9*, 571–577. (b) Warner, A. J.; Lawson, J. R.; Fasano, V.; Ingleson, M. J. Formation of  $\text{C}(\text{sp}^2)$ –Boronate Esters by Borylative Cyclization of Alkynes Using  $\text{BCl}_3$ . *Angew. Chem., Int. Ed.* **2015**, *54*, 11245–11249. (c) Warner, A. J.; Churn, A.; McGough, J. S.; Ingleson, M. J.  $\text{BCl}_3$ –Induced Annulative Oxo- and Thioboration for the Formation of C3–Borylated Benzofurans and Benzothiophenes. *Angew. Chem., Int. Ed.* **2017**, *56*, 354–358. (d) Yuan, K.; Wang, S. *trans*-Aminoboration across Internal Alkynes Catalyzed by  $\text{B}(\text{C}_6\text{F}_5)_3$  for the Synthesis of Borylated Indoles.

*Org. Lett.* **2017**, *19*, 1462–1465. (e) Kirschner, S.; Bao, S.-S.; Fengel, M. K.; Bolte, M.; Lerner, H.-W.; Wagner, M. Aryl–aryl coupling in a polycyclic aromatic hydrocarbon with embedded tetracoordinate boron centre. *Org. Biomol. Chem.* **2019**, *17*, 5060–5065. (f) Radtke, J.; Møllerup, S. K.; Bolte, M.; Lerner, H.-W.; Wang, S.; Wagner, M. Aryl Insertion vs. Aryl–Aryl Coupling in C,C-Chelated Organoborates: the “Missing Link” of Tetraarylborate Photochemistry. *Org. Lett.* **2018**, *20*, 3966–3970. (g) Eisch, J. J.; Tamao, K.; Wilcsek, R. J. Generation of Boracabenoid and Boracyclopropene Intermediates from the Photolysis of Tetraorganoborate Salts in Aprotic Media. *J. Am. Chem. Soc.* **1975**, *97*, 895–897.

(4) (a) Ando, N.; Fukazawa, A.; Kushida, T.; Shiota, Y.; Itoyama, S.; Yoshizawa, K.; Matsui, Y.; Kuramoto, Y.; Ikeda, H.; Yamaguchi, S. Photochemical Intramolecular C–H Addition of Dimesityl(hetero)-arylboranes through a [1,6]-Sigmatropic Rearrangement. *Angew. Chem., Int. Ed.* **2017**, *56*, 12210–12214. (b) Iida, A.; Saito, S.; Sasamori, T.; Yamaguchi, S. Borylated dibenzoborepin: synthesis by skeletal rearrangement and photochromism based on bora-Nazarov cyclization. *Angew. Chem., Int. Ed.* **2013**, *52*, 3760–4. (c) Wang, H.; Zhang, J.; Xie, Z. Reversible Photothermal Isomerization of Carborane-Fused Azaborole to Borirane: Synthesis and Reactivity of Carbene-Stabilized Carborane-Fused Borirane. *Angew. Chem., Int. Ed.* **2017**, *56*, 9198–9201.

(5) (a) He, Z.-C.; Møllerup, S. K.; Liu, L.-J.; Wang, X.; Dao, C.; Wang, S. Reversible Photoisomerization from Borepin to Boratanorcaradiene and Double Aryl Migration from Boron to Carbon. *Angew. Chem., Int. Ed.* **2019**, *58*, 6683–6687. (b) Møllerup, S. K.; Li, C.; Radtke, J.; Wang, X.; Li, Q. S.; Wang, S. Photochemical Generation of Chiral N,B,X-Heterocycles by Heteroaromatic C–X Bond Scission (X = S, O) and Boron Insertion. *Angew. Chem., Int. Ed.* **2018**, *57*, 9634–9639. (c) Radtke, J.; Møllerup, S. K.; Bolte, M.; Lerner, H.-W.; Wang, S.; Wagner, M. Aryl Insertion vs. Aryl–Aryl Coupling in C,C-Chelated Organoborates: the “Missing Link” of Tetraarylborate Photochemistry. *Org. Lett.* **2018**, *20*, 3966–3970. (d) Edel, K.; Krieg, M.; Grote, D.; Bettinger, H. F. Photoreactions of Phenylborylene with Dinitrogen and Carbon Monoxide. *J. Am. Chem. Soc.* **2017**, *139*, 15151–15159. (e) Møllerup, S. K.; Li, C.; Peng, T.; Wang, S. Regioselective Photoisomerization/C–C Bond Formation of Asymmetric B(ppy)(Mes)(Ar): The Role of the Aryl Groups on Boron. *Angew. Chem., Int. Ed.* **2017**, *56*, 6093–6097. (f) Yang, D. T.; Møllerup, S. K.; Peng, J. B.; Wang, X.; Li, Q. S.; Wang, S. Substituent Directed Phototransformations of BN-Heterocycles: Elimination vs Isomerization via Selective B–C Bond Cleavage. *J. Am. Chem. Soc.* **2016**, *138*, 11513–11516.

(6) (a) Rao, Y.-L.; Amarné, H.; Zhao, S. B.; McCormick, T. M.; Martić, S.; Sun, Y.; Wang, R. Y.; Wang, S. Reversible Intramolecular C–C Bond Formation/Breaking and Color Switching Mediated by a N,C-Chelate in (2-ph-py)BMes<sub>2</sub> and (5-BMes<sub>2</sub>-2-ph-py)BMes<sub>2</sub>. *J. Am. Chem. Soc.* **2008**, *130*, 12898–12900. (b) Rao, Y. L.; Amarné, H.; Chen, L. D.; Brown, M. L.; Mosey, N. J.; Wang, S. Photo- and thermal-induced multistructural transformation of 2-phenylazoyl chelate boron compounds. *J. Am. Chem. Soc.* **2013**, *135*, 3407–3410. (c) Rao, Y. L.; Horl, C.; Braunschweig, H.; Wang, S. Reversible photochemical and thermal isomerization of azaboratabisnorcaradiene to azaborabenzotropolidene. *Angew. Chem., Int. Ed.* **2014**, *53*, 9086–9089.

(7) Li, H. J.; Møllerup, S. K.; Wang, X.; Wang, S. Transforming benzylideneamine N,C-chelate boron compounds to BN-cycloocta-/cyclohepta-trienes bearing a tetrasubstituted B = N unit via photoisomerization. *Chem. Commun.* **2018**, *54*, 8245–8248.

(8) Shi, Y.-G.; Møllerup, S. K.; Yuan, K.; Hu, G.-F.; Sauriol, F.; Peng, T.; Wang, N.; Chen, P.; Wang, S. Stabilising fleeting intermediates of stilbene photocyclization with amino-borane functionalisation: the rare isolation of persistent dihydrophenanthrenes and their [1,5] H-shift isomers. *Chem. Sci.* **2018**, *9*, 3844–3855.

(9) Shi, Y. G.; Wang, J. W.; Li, H.; Hu, G. F.; Li, X.; Møllerup, S. K.; Wang, N.; Peng, T.; Wang, S. A simple multi-responsive system based on aldehyde functionalized amino-boranes. *Chem. Sci.* **2018**, *9*, 1902–1911.

(10) Bluer, K. R.; Laperriere, L. E.; Pujol, A.; Yruegas, S.; Adiraju, V. A. K.; Martin, C. D. Coordination and Ring Expansion of 1,2-Dipolar Molecules with 9-Phenyl-9-borafluorene. *Organometallics* **2018**, *37*, 2917–2927.

(11) Neumüller, B.; Gahlmann, F. Diorganoinidiumfluoride. Die Kristallstrukturen von [iPr<sub>2</sub>In(THF)<sub>2</sub>][BF<sub>4</sub>] und (MesBO)<sub>3</sub>. *J. Organomet. Chem.* **1991**, *414*, 271–283.

(12) (a) Loh, Y. K.; Porteous, K.; Fuentes, M. A.; Do, D. C. H.; Hicks, J.; Aldridge, S. An Acid-Free Anionic Oxoborane Isoelectronic with Carbonyl: Facile Access and Transfer of a Terminal B = O Double Bond. *J. Am. Chem. Soc.* **2019**, *141*, 8073–8077. (b) Wang, Y.; Hu, H.; Zhang, J.; Cui, C. Comparison of Anionic and Lewis Acid Stabilized N-Heterocyclic Oxoboranes: Their Facile Synthesis from a Borinic Acid. *Angew. Chem., Int. Ed.* **2011**, *50*, 2816–2819. (c) Swarnakar, A. K.; Hering-Junghans, C.; Ferguson, M. J.; McDonald, R.; Rivard, E. Oxoborane (RBO) Complexation and Concomitant Electrophilic Bond Activation Processes. *Chem. - Eur. J.* **2017**, *23*, 8628–8631.

(13) Wang, P.; Zhou, L.; Zhang, X.; Liang, X. Facilitated photochemical cleavage of benzylic C–O bond. Application to photolabile hydroxyl-protecting group design. *Chem. Commun.* **2010**, *46*, 1514–1516.